Journal of National Fisheries University 45 (2) 47－57 (1996)

Inelastic Stress Analysis of a Steam Generator at Transient Conditions

Kiyokazu Kobatake*1, Keiichi Yoshihara*2, Masanobu Yahiro*3, Satoru Ezoe*4, and Hisayuki Yamaura*1

In designing the steam generators, the designers must consider the operational conditions and make sure the integrity of the components is adequate. The loads to be applied are static and dynamic ones, including thermal transients. This paper shows key portions to be evaluated for the integrity of the structures, and shows an example of the inelastic stress analysis of a steam generator tubesheet.

1 Introduction

The steam generators for the turbine generators have complicated structures, however, they can be shown schematically in Fig.1. The primary coolant, which receives the heat capacity from the heat source, comes into the inlet nozzle of the shell, gives the heat to the feed water through the heat transfer tubes and then goes out from the outlet nozzle. On the other hand, the feed water comes into the water chamber, and flows into the many heat transfer tubes through the tubesheet. Receiving the heat from the primary flow, the secondary flow is evaporated and super-heated, and then goes out from the steam chamber through the outlet tubesheet.

The designers and the system engineers are required to consider the operational conditions and make sure of the structural strength of the steam generators as they will get the static and dynamic loads in whole life. The key portions to be evaluated can be thought of as follows.

(1)Water chamber

a) Loads of the static pressure and the temperature

(2)Heat transfer tubes

a) Stresses due to the thermal expansion differencebetween the tubes and the shell

b) Dynamic responses to the earthquakes

c) Vibration forces due to Karuman vortex

d) Fluctuation of the temperature difference through the tube wall due to the thermal transfer coefficient change of the inside tube surface by the cyclic change of DNB (Departure from Nucleate

水産大学校研究業績 第1549号, 1996年6月19日受付

Contribution from National Fisheries University, No.1549. Received Jun. 19, 1996

*1 Laboratory of Mechanical Engineering I, Department of Marine Engineering, National Fisheries University (水産大学校機関 学科機械工学第一講座).

*2 Laboratory of Marine Steam Engineering, Department of Marine Engineering, National Fisheries University (水産大学校機関学科蒸気原動機講座).

*3 Laboratory of Natural Science, Division of General Education, National Fisheries University (水産大学校教養学科自然科学教室).

*4 Laboratory of Mechanical Engineering II, Department of Marine Engineering, National Fisheries University (水産大学校機関学科機械工学第二講座).

Boiling) point by evaporation

(3)Shell

a) Dynamic responses to earthquakes

b) Thermal transient to the inlet and outlet nozzles

(4)Outlet tubesheet with the steam chamber and the shell

a) Structural discontinuity stresses among the shell, the outlet tubesheet and steam chamber induced by the static loads and the thermal transients

b) Differences of the stiffness at the high temperature between the perforated tubesheet (ligament) and the outside rim of the tubesheet

To satisfy all the requirements of the design specifications and the design criteria, elastic and inelastic analyses are performed, and if necessary, the structural details are modified.

The design criteria of ASME Boiler and Pressure Vessel Code Section III, code case 1592[1] and its revision N-47[2] are based on the philosophy "design by analysis" and require to perform a detailed inelastic analysis if the evaluation by an elastic analysis does not satisfy the requirements[3]. However, for the design by inelastic analysis, the data of the material properties are limited, and for analysis it takes too much manpower. In spite of the various theoretical proposals, there are not so many examples applied to the practical designs[4, 5, 6].

According to authors analytical experiences, one of the most important analyses seems to be the structural discontinuity portions among the shell, the outlet tubesheet and the steam chamber, induced by the static loads and the thermal transients.

This paper shows a practical example of inelastic stress analysis, applied to the shell-tubesheet-steam chamber of a steam generator subjected to a thermal shock, and is written from the point of designing, rather than the theoretical one.

Some useful informations are obtained from the results of the analysis.

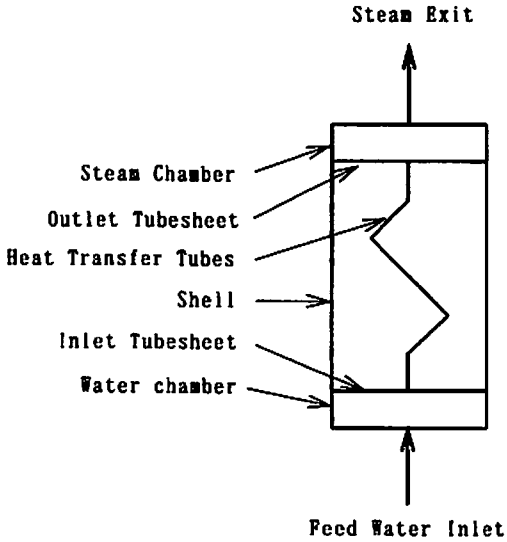

Fig. 1 Schematic drawing of steam generators

2 Analysis Method

Heat exchanger tubesheets of steam generators have generally a complicated configuration and are subjected to severe thermal shock at the transients. An inelastic stress analysis is generally required to show the integrity of the tubesheets in accordance with an available elevated temperature structural design code. However, the application of the detailed inelastic stress analysis to the 3-dimensional tubesheet design is very limited because it entails too much computer calculation hours and manpower. Therefore a simplified inelastic analysis procedure with a reasonable accuracy is required to be developed.

In the case of tubesheets analysis for the elastic design, a hand calculation method has been successfully used on the concept of an equivalent solid plate.

O'Donnell et al employed limit analyses to determine the plastic strength of the perforated plate and studied further the plastic strain concentrations in ligaments[5, 6, 7].

On the other hand, Pai et al have proposed an inelastic analysis procedure of the tubesheets combining the solid plate concept with FEM technique[8]. In spite of the scarce application examples and comparisons with

experimental data of the procedure, the method seems to be a very practical one for the designers. Authers applied this method as mentioned below.

3 Description of the Analysis Model

The applied structure is a superheater tubesheet designed for a LMFBR (Liquid Metal Fast Breeder Reactor) plant of which details are shown in Fig.2. Loading conditions are determined on the basis of an external power failure accident, in which the most effective load is the cold shock at a sodium (primary coolant) flow transient. Other loads are internal pressure, flange bolt forces, and tube reaction forces due to the cold shock. The totalized loading histories for the analysis are shown schematically in Fig.3. The postulated life

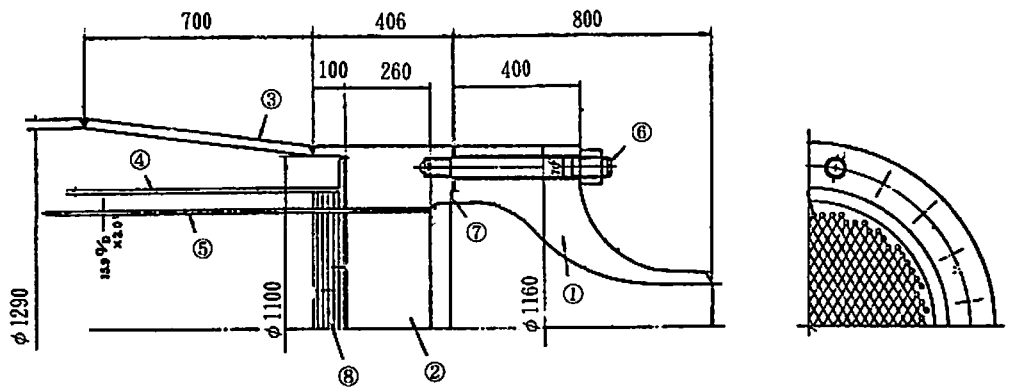

①Steam chamber ②Tubesheet ③Shell ④Sleeve ⑤Tubes ⑥Bolts ⑦Gasket ⑧Buffer

Fig. 2 Detailed Drawing of the Tubesheet

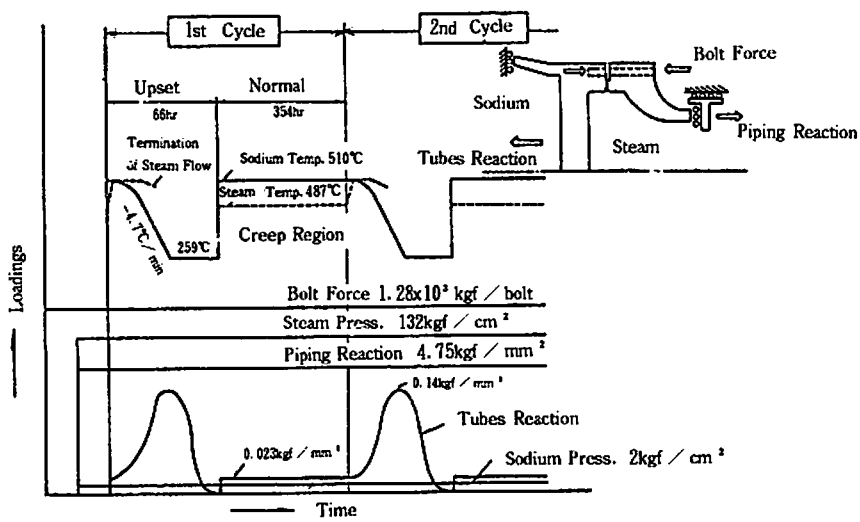

Fig. 3 Schematic loading history

time is 2.1×10^5 hours and the accident is supposed to be cycled 500times, which corresponds to 420 hrs/cycle. The analysis has been performed for the first two cycles. The material of the component is 304SS and the material data for the analysis are mainly taken from Ref.1 and 2.

4 Theory and Procedure of Analysis

4.1 Basic Theory and Analysis Computer Code

FEM technique based on the recommended theory[9] is adopted, which consists of the kinematic work hardening rule for plasticity and the equation of the state method for creep. All the elements used are of 8-node quadratic elements (3 x 3 Gaussian integral points). A two-dimensional axisymmetric inelastic analysis programme "KINE-T"[10] is used in the following analysis, which was developed by one of the authors and the colleagues.

4.2 Analysis Procedure

The analysis procedure has been developed for the inelastic analysis of tubesheets using the finite element technique[8]. Basically, this approach is an extension of the equivalent solid plate concept and consists of the following 3 analytical steps.

Step 1 : Determine the effective elastic-plastic and creep properties of the perforated plate, using a repetitive segment of the hole array.

Step 2 : Analyze the global structure in which the tubesheet is replaced by an equivalent solid plate.

Step 3 : Analyze the tubesheet itself in detail, using the boundary traction derived from the results obtained in step 2.

4.3 Analysis

Step 1. Determination of Effective Properties of Tubesheet

The hole array of the tubesheet is an equilateral triangular pattern with pitch P=29mm, minimum ligament width h=17.5mm (which gives the ligament efficiency $\eta = 0.603$). Thickness of the sheet t is 260mm. The effective properties for the six loading conditions[11] are derived. However, in the present analysis, the representative X and Y directional properties are calculated and the average values between them are used as effective properties. Calculations are performed under the generalized plane strain condition using the mesh division.

The effective elastic-plastic and creep properties are obtained as shown in Fig.4 and Fig. 5. Both plastic and creep strength in Y-direction is stronger than that of X-direction. Basic creep data of 304SS are taken from Ref. 12. The effective creep equation is obtained as follows.

$$\varepsilon_c = A\sigma^{B\sigma+C} \cdot t^{D\sigma^2+E\sigma+F} \times 10^{-2}(\%)$$

$A = 0.71844 \times 10^{-8}$ $D = -0.35309 \times 10^{-2}$

$B = -0.36857 \times 10^{-1}$ $E = 0.85950 \times 10^{-2}$

$C = 0.69499 \times 10^{1}$ $F = 0.97226$

Results in Step 1 are summarized in Table 1.

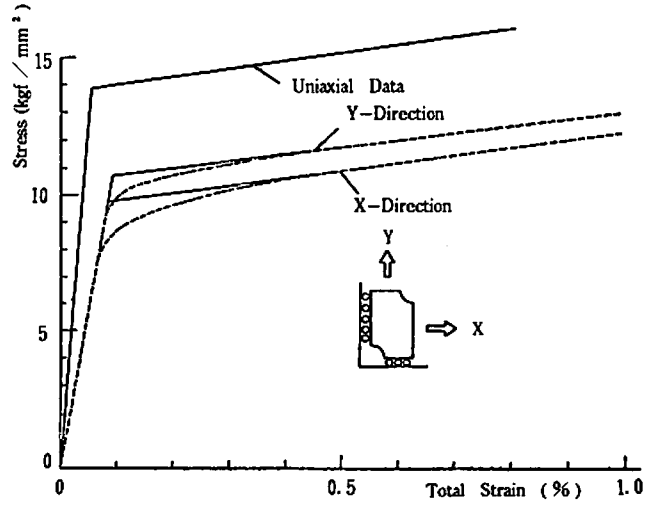

Fig. 4 Effective plastic properties at the conditions of generaliged plane strain and temperature 487℃

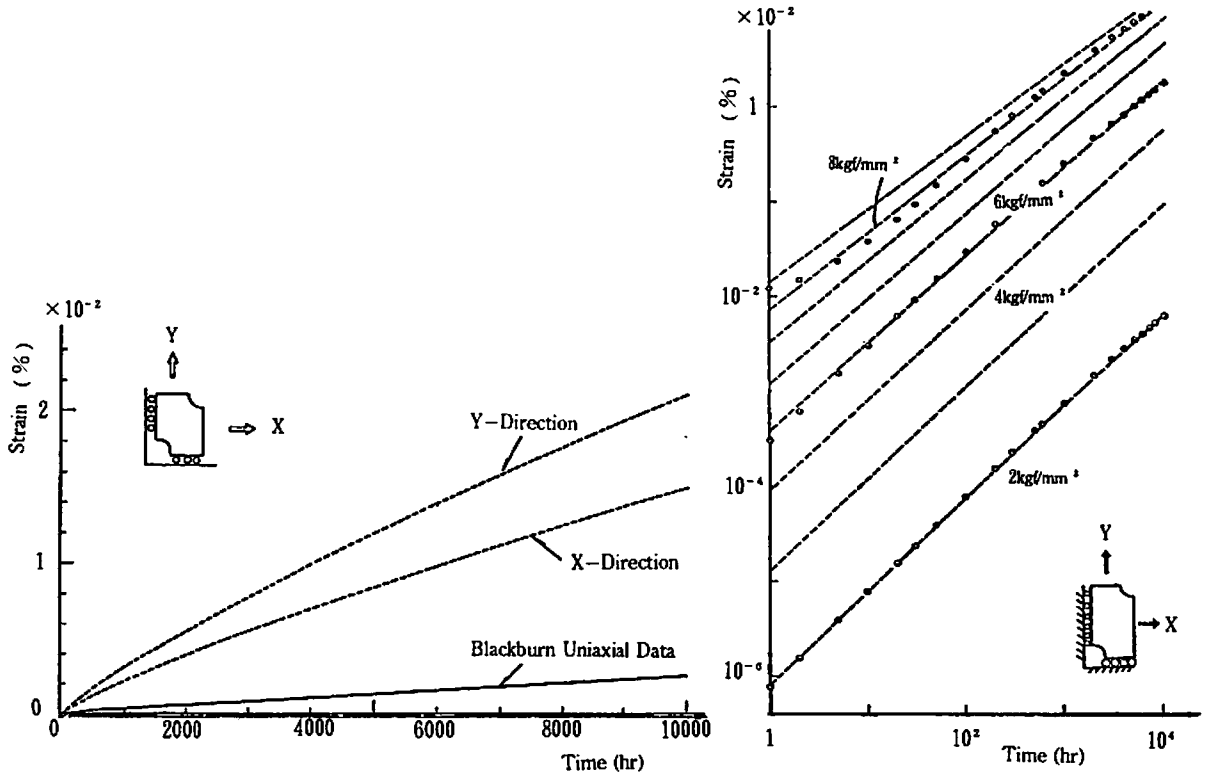

(a) Effective creep strains in X and Y directions at 5kgf/㎟

(b) The average values between effective creep strains of X and Y directions

Fig. 5 Effective creep properties on the generalized plane strain condition at 487℃

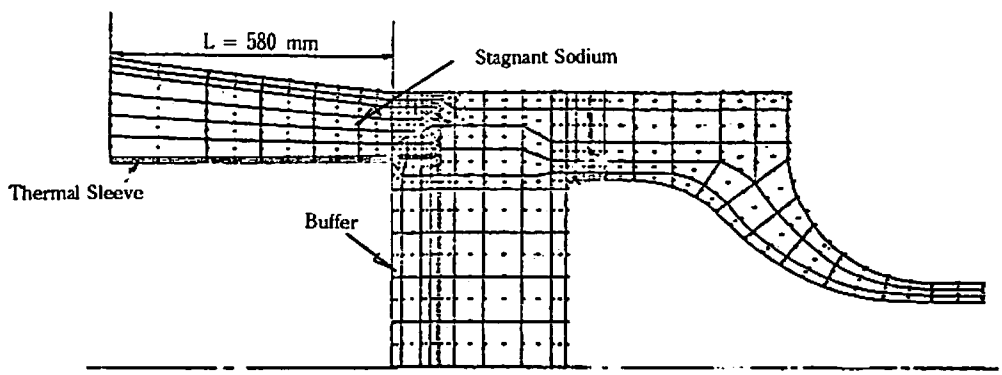

Fig. 6 Axisymmetric Model for global Analysis

Step 2. Global Analysis by Axisymmetric Model

The global analysis is carried out by the mesh division of the axisymmetric model shown in Fig. 6. The typical temperature distributions at the cold shock transient are shown in Fig. 7. The Strain distributions are shown in Fig. 8, where discontinuity portions developed into plastic regime. Fig. 9 shows the strain distributions in the wall thickness direction of the tubesheet, where the maximum plastic strain developed.

From Fig. 7 through Fig. 9, it is seen that the tubesheet is subjected to bending load caused by temperature difference between both sides, and the shake down occurs on the sodium side surface. Creep effect is very small throughout the tubesheet.

Step 3. Analysis of the repetitive of the hole array

The aforementioned global analysis showed that the maximam plastic strain in the tubesheet was induced at the sodium side surface of the sheet-center. Therefore, in the next segment analysis, this localized portion is to be analyzed using the same mesh model of Step 1.

The boundary traction used in Step 3 is the equivalent stresses induced at the localized portion in Step 2 and are shown in Fig. 10. The forces in Fig. 10 are applied equibiaxially to the segment model. Steam transient and steam pressure loads are also considered in Step 3.

As the maximum plastic strain is induced at the surface of the sheet, the segment is analayzed under the plane stress condition.

Fig. 11 shows the progressive plastic zone and Fig. 12 shows a stress-strain curve at a representative point in segment. From these figures, almost all portions develop into plastic regime during the first cycle. But for all subsequent cycles shakedown occurs. The creep effects are negligibly small.

Table 1 Material properties

	304SS	Equivalent Solid
Young's Modulas	1.72×10^4 kgf/mm^2	1.72×10^4 kgf/mm^2
Poisson's Ratio	0.3	0.297
Yield Strength	$(\sigma_Y - 9.4091)(T+164.43)=2893.94$ kgf/mm^2	$\sigma_Y^* = 0.7362\,\sigma_Y$ kgf/mm^2
Work Hardening Coefficient	363.21 kgf/mm^2	285.83 kgf/mm^2
Creep Equation	Blackburn type Creep Equation Ref.[12]	$\varepsilon_c = (A\,\sigma^{B\sigma+C}\,t^{D\sigma^2+E\sigma+F}) \times 10^{-2}$ % $A = 0.71844 \times 10^{-8}$ $B = -0.36857 \times 10^{-1}$ $C = 6.9499$ $D = -0.35309 \times 10^{-2}$ $E = 0.85950 \times 10^{-2}$ $F = 0.972257$ (At 487 ℃)
Thermal Expansion Coefficient	17.95×10^{-6} 1/℃	17.95×10^{-6} 1/℃

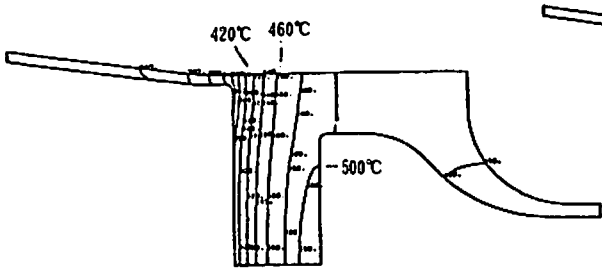

Fig. 7 Temperature distributions during transient

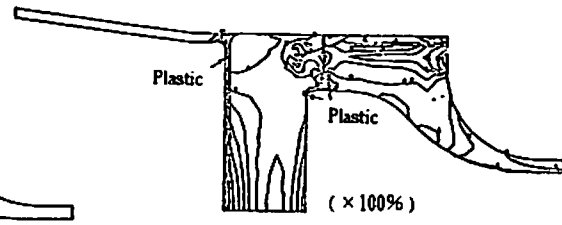

Fig. 8 Strain distributions during transient

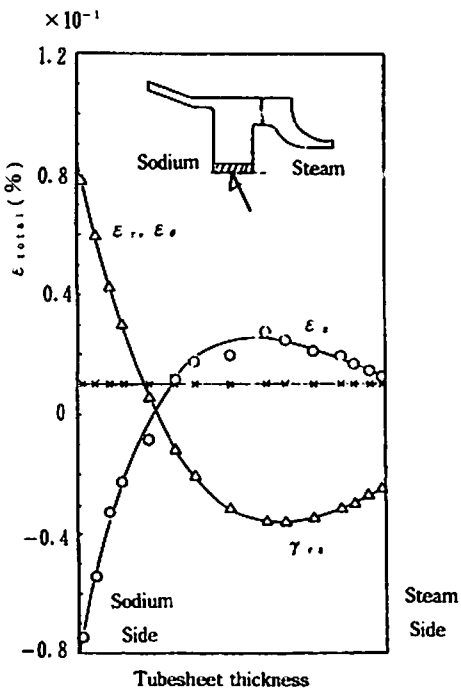

Fig. 9 Strain distributions in the tubesheet

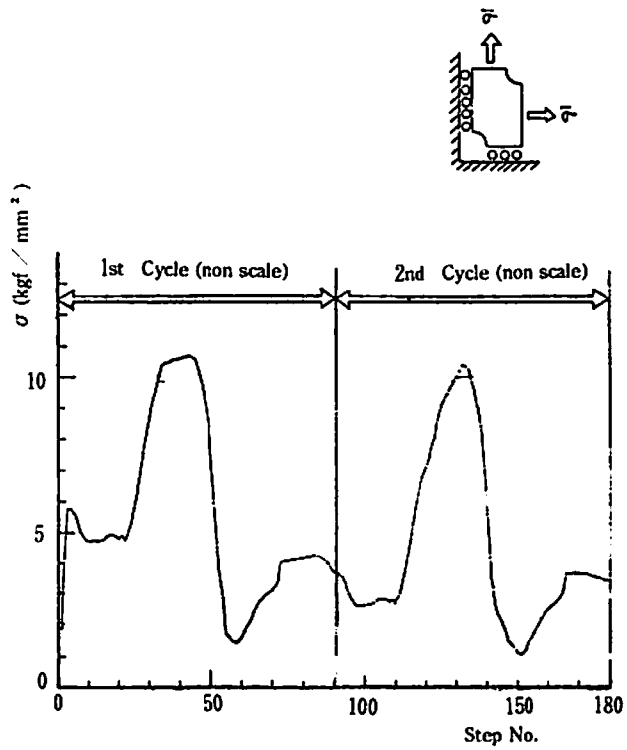

Fig. 10 Boundary traction

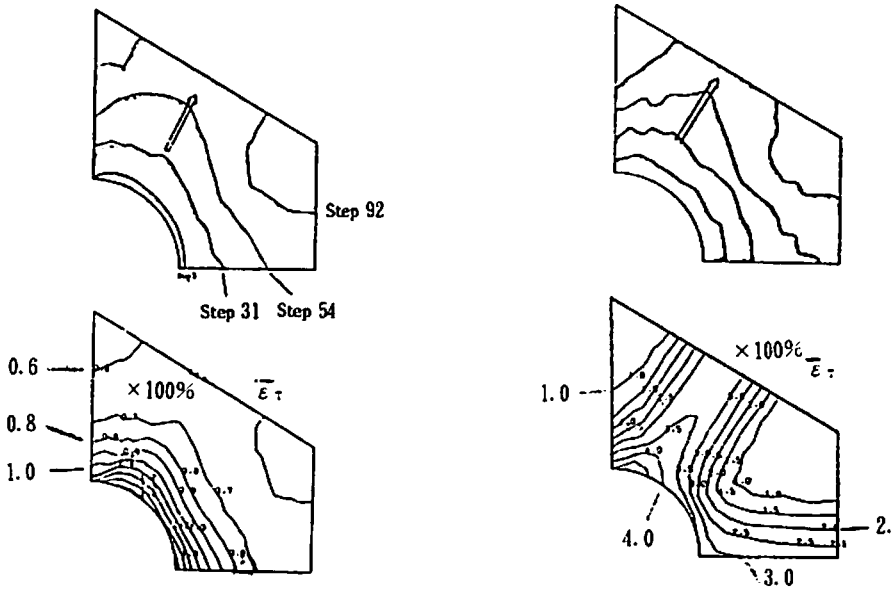

(a) For equibiaxial loading (b) For practical loading

Fig. 11 Progressive plastic zones

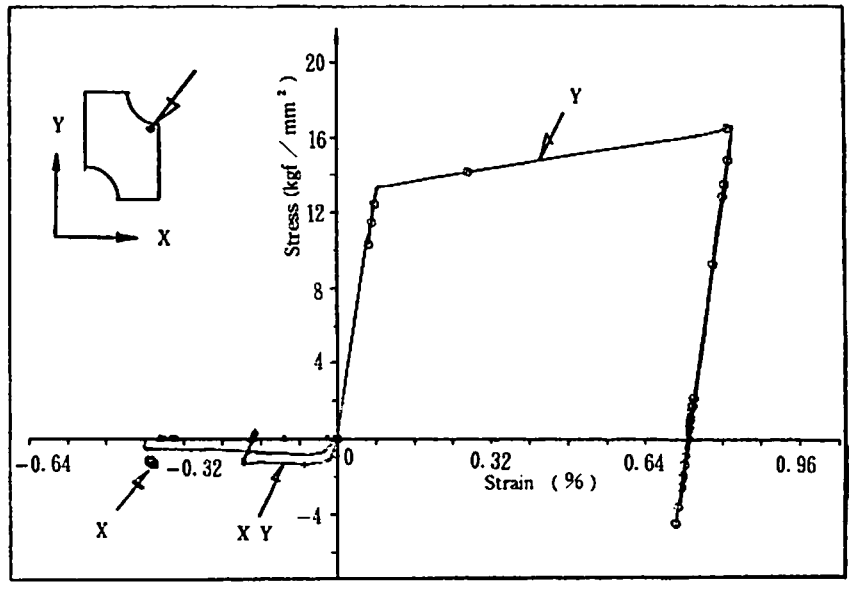

Fig. 12 Stress-strain curve at local point

5 Discussions

Due to the effect of a thermal buffer on moderating the thermal shock, large peak strains did not occur in the tubesheet in Step 2.

As can be seen from the strain distributions in the wall thickness in Fig. 9, the peak strains occurred on the sodium side surface of the tubesheet. The main reason for the strains in the tubesheet was the bending load due to the temperature difference between both sides of the tubesheet. A typical shakedown occurred on the sodium side of the tubesheet as shown in Fig. 12.

Corresponding to these global behavior, almost all portions of the segment developed into the plastic regime during the first cycle and then the shakedown occurred at the second cycle.

The creep effect was so small in both results of the global and the segment analyses, that could be neglected in the practical design.

The inelastic behavior in the vicinity of the hole was studied by using a strain concentraition factor K, which is defined herein as follows.

$$K = \frac{\text{Maximum Peak Strain (elastic + plastic)}}{\text{Effective Strain (elastic + plastic)}} = \frac{\varepsilon_{peak}}{\varepsilon^*}$$

$$\varepsilon^* = \frac{\sqrt{3}}{2}(\varepsilon_x^{*2} + \varepsilon_y^{*2} + (\varepsilon_x^* - \varepsilon_y^*)^2)^{1/2}$$

Fig. 13 shows K versus ε^* curve obtained in Step 3. The dotted line in the same figure is the curve for the pure equibiaxial loading, which is calculated separately by using the same model in order to investigate the basic characteristic of the segment, where $\sigma_y = 14.0 kgf/mm^2$ constant, other properties are same to those in Table 1.

It is noted here that the peak strain is not arised at the hole boundary but at the integral point nearest to the boundary. K increases as the loading progresses deeper into the plastic regime, and tends to stabilize when gross yielding occurs in the segment. In addition, the local location where the peak strain occurs changes as the loading increases.

The charcteristic state of plastic regime development and K versus ε^* curve of the practical loadings are similiar to those of the equibiaxial loading in Fig. 11 and Fig. 13. But the maximum K (=3.0) of the former is greater than that of the latter. As a matter of course, K depends on the ratio of each loading and material properties, especially the temperature dependency of the yield strength.

Therefore, in such a practical design, it seems very important to accummulate many analytical examples for the estimation of K, in addition to the basic uniaxial and equibiaxial loading studies[13), 14)].

The results of the present analysis met the design criteria required in code case 1592 and N-47. The tubes fixed to the tubesheet are neglected in the analysis. The tubes might be needed to consider further in the analysis procedure.

6 Conclusions

Tubesheets subjected to severe thermal loadings, such as LMFBR steam generators, are required to perform a detailed inelastic stress analysis for the confirmation of the structural integrity. Due to the high cost associated with the detailed inelastic analysis, it is necessary to develop a simplified method with a reasonable accuracy. To answer such a need, Pai et al proposed an analytical method. As discussed in this paper, the proposed method shows a very practical one and can be applicable to a full sized model. The example described in this paper will support the design analyses.

Acknowledgement

Authers are indeted to the useful discussions with Mr. Shigeru Takahashi of Kawasaki Heavy Industries.

References

1) ASME : B & PVC, Section III Nuclear Power Plant Components and Code Case 1592.
2) ASME : B&PVC Code Case N-47-29, (1990).
3) K. kobatake and H. Yamaura : J. National Fish. Univ. 44(1), 25-45 (1995).
4) F. A. Simonen et al, Calculations of Steam

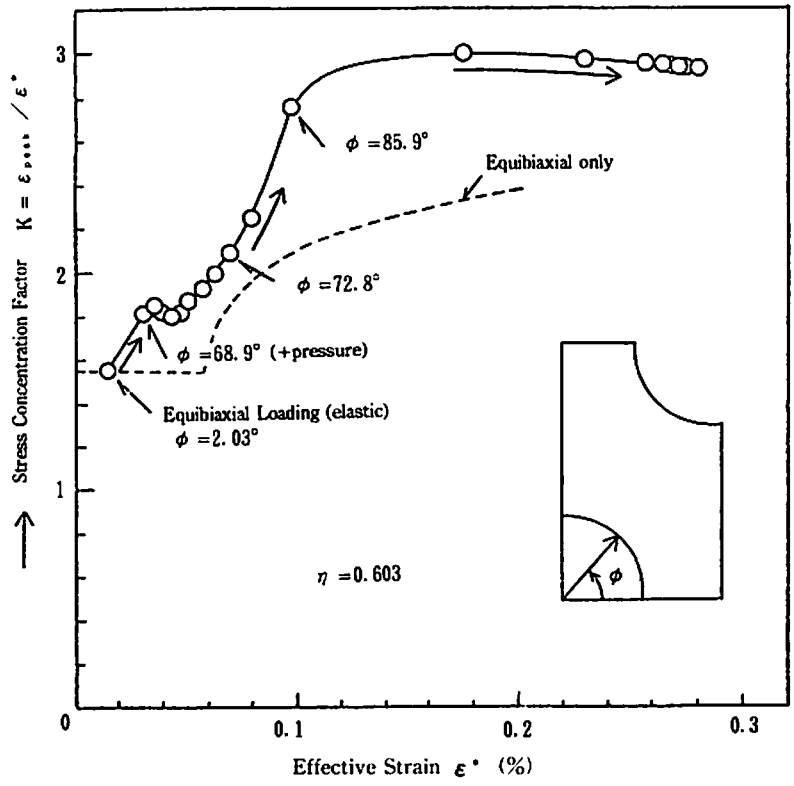

Fig. 13 Strain concentration factor

Genera tor Tube Support Plate Motions Including Interactions with Tubes, ASME PVP-VOL. 318, 73-82 (1995).

5) J. Porowski and W. J. O' Donnell : Plastic Strength of Perforated Plates with Square Penetration Patterns, Trans. ASME ,Journal of Pressure Vessel Technology, 97, J3, 146-154 (1975).

6) J. Porowski and W. J. O' Donnell : Plastic Strain Concen-trations in Ligaments, ASME 76-PVP-32, (1976).

7) D. P. Jones et al : Elastic-Plastic Analysis of Perforated Plates Containing Triangular Penetration Patterns of 10% Ligament Efficiency, ASME 76-PVP-22, (1976).

8) D. H. Pai and M. B. Hsu : Inelastic Analysis of Tubesheets by the Finite Element Method, ASME 75-PVP-57, (1975).

9) O. E. Pugh, et al : Currently Recommended Constitutive Equations for Inelastic Design Analysis of FFTF Components, ORNL-TM-3602, (1972).

10) K. kobatake, S. Takahashi and M. Suzuki : Devlopment of an inelastic stress analysis code "KINE-T" and its Evaluations, SMIRT M1(5),1-12 (1977).

11) T. Slot and T. R. Branca : On the Determination of Effective Elastic Properties for the Equivalent Solid Analysis of Tubesheets, Trans. ASME, Journal of Pressure Vessel Tecnology, 96, J3, 151-160 (1974).

12) Z. Zudns : Elastic-Plastic Creep Response of Structures under Composit Time History of Loadings, The Franklin Institute Research Laboratories, (1975).

13) D. K. Williams et al, 3 Dimensional Stress Evaluation of a Thick Plate with 3 Penetrations Subjected to Pressure and Edge Moment Loadings, PVP-VOL. 301, 201-208 (1995).

14) H. Hirayama et al, Creep-Fatigue Evaluation Rules in Design and DFBR in Japan, PVP-Vol. 313-2, 439-456 (1995)

蒸気発生器の過渡状態に対する非弾性応力解析

小畑滑和・吉原計一・八尋正信・江副　覚・山浦寿幸

発電蒸気タービン用蒸気発生器の設計において、システム設計者ならびに構造解析者は、全寿命中の運転状態を充分に配慮した構造強度を予め検証することが要求される。ここでは、蒸気発生器で特に注目すべき構造部分を摘出し、そのうちで重要な管板とその周辺部分に対する過度状態の非弾性解析を実施し、設計解析者に実施可能な簡易的な非弾性解析法を検討した結果、有効な方法であることが明らかになった。